Transcriptome profiling reveals the role of ZBTB38 knock-down in human neuroblastoma

Jie Chen [1], Chaofeng Xing [1], Li Yan [2], Yabing Wang [3], Haosen Wang [4], Zengmeng Zhang [1], Daolun Yu [1], Jie Li [1], Honglin Li [5], Jun Li [1], Yafei Cai [Corresp. 1]

[1] Anhui Normal University, WuHu, China

[2] Linyi People Hospital, Nanjing, China

[3] The First Affiliated Hospital of Wannan Medical College, WuHu, China

[4] Taizhou 4th Hospital, Taizhou, China

[5] Medical College of Georgia, Augusta State University, Augusta, United States

Corresponding Author: Yafei Cai
Email address: ycai@njau.edu.cn

ZBTB38 belongs to the zinc finger protein family and contains the typical BTB domains. As a transcription factor, ZBTB38 is involved in cell regulation, proliferation and apoptosis, whereas, functional deficiency of ZBTB38 induces the human neuroblastoma cell death potentially. To have some insight into the role of ZBTB38 in neuroblastoma development, high throughput RNA sequencing was performed using the human neuroblastoma cell line SH-SY5Y with the deletion of ZBTB38. In the present study, 2,438 differentially expressed genes (DEGs) in ZBTB38$^{-/-}$ SH-SY5Y cells were obtained, 83.5% of which was down-regulated. Functional annotation of the DEGs in the Kyoto Encyclopedia of Genes and Genomes database revealed that most of the identified genes were enriched in the neurotrophin TRK receptor signaling pathway, including PI3K/Akt and MAPK signaling pathway. we also observed that ZBTB38 affects expression of CDK4/6, Cyclin E, MDM2, ATM, ATR, PTEN,Gadd45 and PIGs in the p53 signaling pathway. In addition, ZBTB38 knockdown significantly suppresses the expression of autophagy-related key genes including PIK3C2A and RB1CC1. The present meeting provides evidence to molecular mechanism of ZBTB38 modulating neuroblastoma development and targeted anti-tumor therapies.

Transcriptome Profiling Reveals the Role of ZBTB38 Knock-down in Human Neuroblastoma

1 Jie Chen[1, 2, 3], Chaofeng Xing[1, 2, †], Li Yan[4], Yabing Wang[5], Haosen Wang[6], Zengmeng Zhang[1], Daolun Yu[1], Jie Li[1], Honglin Li[7], Jun Li[1*], Yafei Cai[1,2*]

[1] College of Life Sciences, Anhui Provincial Key Lab of the Conservation and Exploitation of Biological Resources, Anhui Normal University, Wuhu 241000, China

[2] College of Animal Science and Technology, Nanjing Agricultural University, Nanjing 210095, China

[3] The Secondary Hospital of Wuhu, Wuhu241000, China

[4] Department of Radiation Oncology, Linyi People Hospital, 276003, China

[5] The First Affiliated Hospital of Wannan Medical College, Wuhu241001, China

[6] Taizhou 4th Hospital, Taizhou235300, China

[7] Department of Biochemistry and Molecular Biology, Medical College of Georgia, Augusta University,Augusta, GA 30912, USA

[†] Co-first author

*Corresponding Author:

Jun Li[1], Yafei Cai[1,2]

[1] College of Life Sciences, Anhui Provincial Key Lab of the Conservation and Exploitation of Biological Resources, Anhui Normal University, Wuhu 241000, China

[2] College of Animal Science and Technology, Nanjing Agricultural University, Nanjing 210095, China

Email address: ycai@njau.edu.cn (Y.C.); lijunplant@163.com (J.L.) Tel.: +86-553-386-9297

ABSTRACT

27 ZBTB38 belongs to the zinc finger protein family and contains the typical BTB domains. As a
28 transcription factor, ZBTB38 is involved in cell regulation, proliferation and apoptosis, whereas,
29 functional deficiency of ZBTB38 induces the human neuroblastoma cell death potentially. To
30 have some insight into the role of ZBTB38 in neuroblastoma development, high throughput
31 RNA sequencing was performed using the human neuroblastoma cell line SH-SY5Y with the
32 deletion of ZBTB38. In the present study, 2,438 differentially expressed genes (DEGs) in
33 ZBTB38-/- SH-SY5Y cells were obtained, 83.5% of which was down-regulated. Functional
34 annotation of the DEGs in the Kyoto Encyclopedia of Genes and Genomes database revealed
35 that most of the identified genes were enriched in the neurotrophin TRK receptor signaling
36 pathway, including PI3K/Akt and MAPK signaling pathway. we also observed that ZBTB38
37 affects expression of CDK4/6, Cyclin E, MDM2, ATM, ATR, PTEN,Gadd45 and PIGs in the
38 p53 signaling pathway. In addition, ZBTB38 knockdown significantly suppresses the expression
39 of autophagy-related key genes including PIK3C2A and RB1CC1. The present meeting provides
40 evidence to molecular mechanism of ZBTB38 modulating neuroblastoma development and
41 targeted anti-tumor therapies.

INTRODUCTION

43 Neuroblastoma (NB) is an embryonal malignant tumor that originated from neural crest cells of
44 the sympathetic nervous system. It is the most common extracranial solid tumor in children,
45 accounting for 8-10% of pediatric malignancies (Castel et al. 2013; Schulte et al. 2013). This
46 disease is highly malignant and progresses rapidly–most of the patients would have been at the
47 advanced stage upon diagnosis when conventional radiotherapy and chemotherapy would have
48 little efficacy, so their survival rate is very low (Bagatell & Cohn 2016). In recent years, new
49 therapeutic methods including hematopoietic stem cell transplantation and biological
50   immunotherapy have been employed to treat relapsed or refractory NB, but the efficacy is still
51 limited (Binkhathlan & Lavasanifar 2013; Han & Wang 2015). Drug resistance has been
52 recognized as the key obstacle to reach a satisfactory outcome (Castel et al. 2013), while
53 induction of programmed death of the cancer cells by targeted gene therapy shows great potential
54 in improving the cure rate and long-term survival of NB patients, especially those with higher
55 risks.

56 ZBTB38 belongs to the zinc finger and BTB domain-containing protein family. Most members
57 of the family, as transcription factors, bind to specific DNA sequences and regulate the
58 transcriptional activity of target genes (Sasai et al. 2005; Stogios et al. 2005). In addition, the
59 family members also involve in various intracellular signal transduction pathways via
60 recognizing and interacting with other proteins, thereby playing important roles in the
61 transcriptional repression, DNA damage, tumorigenesis, and cell proliferation, differentiation,
62 and apoptosis (Lee et al. 2010; Matsuda et al. 2008; Nishii et al. 2012). At least 49 ZBTB
63 proteins are encoded in the human genome, most of which are nuclear proteins (Lee & Maeda
64 2012). Among the predicted BTB domain-containing proteins encoded by the human genome,
65 only several of them have been functionally characterized (Cai et al. 2012; Matsuda et al. 2008).
66 No relevant studies have been reported concerning the effect of ZBTB38 in human
67 neuroblastoma.

68 Transcriptomic studies are developing rapidly over recent years, which, contrary to the studies
69 on an individual gene, enable the investigation on the altered expression of differentially
70 expressed genes (DEGs) on the level of whole protein-coding or non-coding RNAs in cells or
71 tissues of the body. Besides, it can also provide information of the relationship between
72 transcriptional regulation and the protein functions in the whole genome under specific
73 conditions (Reimann et al. 2014; Zhao et al. 2011). Next-generation sequencing (NGS)
74 technology offers important technical support for the annotation and quantification of
75 transcriptomes. The major strength of this technique lies in its high-throughput and high
76 sensitivity for transcript abundance, providing throughout understanding of the transcriptional
77 information of the genome in a comprehensive manner and valuable resources for studies
78 investigating therapeutic biomarkers of cance (Chang et al. 2015; Li et al. 2014).

79 Therefore, in the present study, a high-throughput transcriptome sequencing approach was
80 adopted to investigate the transcriptome profiles of neuroblastoma cells in which the expression
81 of ZBTB38 gene was down-regulated, thus revealing potential biomarkers associated with anti-
82 tumor therapies in neuroblastoma.

83 ## MATERIALS & METHODS

84 ### *Cell culture and standard assays*

85 SH-SY5Y cells were purchased from American Type Culture Collection (Rockville, MD, USA)
86 and cultured in Dulbecco's modified Eagle's medium supplemented with 10% fetal bovine
87 serum and penicillin–streptomycin. Transient transfections, quantitative real-time polymerase

88   chain reaction (qRT-PCR) and western blotting were performed as described previously (Cai et

89   al. 2012; Cai et al. 2017). The primers used in qRT-PCR and siRNA suppression assays are

90   listed in supplemental Table S1. Cell viability was tested using the CCK-8 assay. The absorbance

91   of each well was measured at 450 nm on a microplate reader. The proliferation rate was defined

92   in terms of the percentage of each group of surviving cells compared with the untreated group for

93   both cell lines.

94   ***RNA Preparation and library construction for transcriptome sequencing***

95   Transcriptome high-throughput sequencing was performed in the control group (SH-SY5Y cells

96   transfected with liposome alone, Samples-ID: T04, T05, T06) and the treatment group (SH-

97   SY5Y cells transfected with ZBTB38 siRNA, Samples-ID: T01, T02, T07). Total RNA was

98   isolated from SH-SY5Y cells using TRIzol and the pure-link RNA mini kit (ThermoFisher

99   Scientific, Waltham, MA, USA) according to manufacturer's instructions. RNA purity was

100   checked using the NanoPhotometer spectrophotometer (IMPLEN, CA, USA). RNA

101   concentration was measured using the Qubit RNA Assay Kit in Qubit 2.0 Fluorometer (Life

102   Technologies, CA, USA). RNA integrity was assessed using the RNA Nano 6000 Assay Kit of

103   the Agilent Bioanalyzer 2100 system (Agilent Technologies, CA, USA).

104   In total, 2 µg RNA per sample was used as input material for RNA sample preparations. This

105   study included two groups of three biological replicates. Sequencing libraries were generated

106   using a NEBNext UltraTM RNA Library Prep Kit for Illumina (NEB, USA), and index codes

107   were added to attribute sequences to each sample. Fragmentation was performed using divalent

108   cations under elevated temperature in NEBNext First Strand Synthesis Reaction Buffer (5×).

109   First-strand cDNA was synthesized using random hexamer primer and M-MuLV Reverse

110   Transcriptase (RNase H). Second-strand cDNA synthesis was subsequently performed using

111   DNA Polymerase I and RNase H. Remaining overhangs were converted into blunt ends via

112   exonuclease/polymerase activities. After the adenylation of 3′ ends of DNA fragments, NEBNext

113   Adaptor with a hairpin loop structure was ligated to prepare for hybridization. The library

114   fragments were purified using AMPure XP system (Beckman Coulter, Beverly, USA). Then, 3

115   µl USER Enzyme (NEB, USA) was used with size-selected, adaptor-ligated cDNA at 37°C for

116   15 min, followed by 5 min at 95°C before PCR. Following this, PCR was performed with

117   Phusion High-Fidelity DNA polymerase, universal PCR primers, and index (X) Primer. Finally,

118   PCR products were purified (AMPure XP system), and library quality was assessed using the

119   Agilent Bioanalyzer 2100 system. The clustering of the index-coded samples was performed on a

120   cBot Cluster Generation System using the TruSeq PE Cluster Kit v4-cBot-HS (Illumia).

121   Following cluster generation, the library preparations were sequenced on an Illumina Hiseq 2500
122   platform, and paired-end reads were generated.

123   **_Data and Statistical Analysis_**

124   *Cancer genomics analysis*

125   we downloaded the mRNA expression data from TCGA ([The Cancer Genome Atlas](#))database
126   and systematically evaluated the expression of ZBTB38 and correlation with patients' survival in
127   511 brain lower grade glioma samples of the TCGA database.

128   *Quality control*

129   Raw reads of fastq format were firstly processed through in-house perl scripts. In this step, clean
130   reads were obtained by removing reads containing adapter, reads containing ploy-N and low
131   quality reads from raw reads. At the same time, Q20, Q30, GC-content and sequence duplication
132   level of the clean reads were calculated. All the downstream analyses were based on clean reads
133   with high quality (Ewing & Green 1998; Ewing et al. 1998). The clean data of this article are
134   publicly available in the NCBI Sequence Reads Archive (SRA) with accession number
135   SRP150042.

136   *Comparative analysis*

137   The adaptor sequences and low-quality sequence reads were removed from the data sets. Raw
138   sequences were transformed into clean reads after data processing. These clean reads were then
139   mapped to the reference genome sequence. Only reads with a perfect match or one mismatch
140   were further analyzed and annotated based on the reference genome. Tophat2 tools soft were
141   used to map with reference genome (Kim et al. 2013; Langmead et al. 2009). Reference genome
142   download address:[ftp://ftp.ensembl.org/pub/release-80/fasta/homo_sapiens/.](#)

143   *Gene functional annotation*

144   The assembled sequences were compared against the NR ([NCBI non-redundant protein](#)
145   [sequences](#)), Pfam ([Protein family](#)), KOG/COG ([Clusters of Orthologous Groups of proteins](#)),
146   Swiss-Prot ([A manually annotated and reviewed protein sequence database](#)), KO ([KEGG](#)
147   [Ortholog database](#)), and GO ([Gene Ontology](#)) databases with an E-value $\leq 10^{-5}$ for the functional
148   annotation. The Blast2GO program was used to obtain GO annotation of unigenes including
149   molecular function, biological process, and cellular component categories (Gotz et al. 2008).

150   *Differential expression analysis*

151 Differential expression analysis of the two conditions was performed using the DEGseq R

152 package (Robinson et al. 2010). The P-values obtained from a negative binomial model of gene

153 expression were adjusted using Benjamini and Hochberg corrections to control for false

154 discovery rates (Anders & Huber 2010). Genes with an adjusted P-value < 0.05 were considered

155 to be differently expressed between groups. DEG expression levels were estimated by fragments

156 per kilobase of transcript per million fragments mapped (Florea et al. 2013). The formula is

157 shown as follow:

158
$$FPKM = \frac{cDNA\ Fragments}{Mapped\ Fragments(Millions) \times Transcript\ Length(kb)}$$

159 *GO enrichment and KEGG pathway enrichment analysis*

160 GO enrichment analysis of the differently expressed genes (DEGs) was implemented in the

161 "GOseq" package in R based on a Wallenius non-central hyper-geometric distribution, which

162 can adjust for gene length bias in DEGs (Young et al. 2010).

163 KEGG is a database for understanding high-level functions and utilities of biological systems

164 through large-scale molecular datasets generated by genome sequencing and other high-

165 throughput experimental technologies (http://www.genome.jp/kegg/) (Kanehisa et al. 2008). We

166 used the KOBAS software to test for the statistical enrichment of differentially expressed genes

167 in KEGG pathways. KEGG enrichment can identify the principal metabolic pathways and signal

168 transduction pathways of DEGs (Mao et al. 2005).

169 *DEGs quantitative real-time pcr (qRT-PCR) verification*

170 For validation of the transcriptome result, we subjected three significantly differential expressed

171 unigenes on related pathways to qRT-PCR analysis. Redundant RNA from the cDNA library

172 preparation was used to perform reverse transcription according to the Invitrogen protocol.

173 quantitative real-time polymerase chain reaction (qRT-PCR) were performed as described

174 previously (Zhang et al. 2017). The primers used in qRT-PCR suppression assays are listed in

175 *Table S1*.

176 *Statistical analysis*

177 All data were reported as mean ± standard deviation and analyzed using one-way analysis of

178 variance in SPSS v.17.0. Statistical tests were performed with the Kruskal–Wallis and Mann–

179 Whitney U-tests. A least significant difference test was used for comparisons between groups. A

180 P-value < 0.05 was considered statistically significant.

RESULTS

181

Variation of ZBTB38 in tumors

182

According to the statistical analysis of the TCGAdatabase resources, we found that the

183

expression changes of ZBTB38 gene are closely related to the occurrence of 20 kinds of cancers,

184

and especially the most remarkable down-regulated expression in UCEC (Uterine corpus

185

endometrial carcinoma) and CESC (Cervical squamous cell carcinoma and endocervical

186

adenocarcinoma) (*Fig. 1*). And wealso uncover here that low expression of ZBTB38 was

187

associated with improved the prognosis of the LGG (Brain lower grade glioma) patients (*Fig. 2*),

188

suggesting that these changes are closely related to neuronal tumors.

189

Neuroblastoma cell proliferation and viability after down-regulated of ZBTB38 expression

190

To investigate the importance of ZBTB38 in theprocess of neuronal tumors, three pairs of

191

siRNAs named siRNA1, siRNA2, and siRNA3, were designed to suppress expression of

192

ZBTB38 in human neuroblastoma cells SH-SY5Y. The protein level of ZBTB38 was decreased

193

significantly ($p < 0.05$) at 24 h after transfection (*Fig. 3A and B*), and furthermore, siRNA3

194

worked best for the suppression. No significant difference in cell proliferation and viability was

195

observed among the initial phases of each group after culture by transient transfection ($p > 0.05$).

196

From 12–72 h, the ZBTB38$^{-/-}$ SH-SY5Y group showed significantly lower cell proliferation and

197

viability than the control group ($p < 0.05$) (*Fig. 3C and D*).

198

Quality control and yield statistics of transcriptome sequencing data

199

A total of 47.05 Gb clean data were obtained through the transcriptome sequencing of SH-SY5Y

200

cells, with at least 6.12 Gb and a ≥89.30% Q30 percentage for each sample (*Table 1*). Efficiency

201

of sequence alignment referred to the percentage of mapped reads in the clean reads, which

202

reflected the utilization of transcriptome sequencing data. Statistical analysis of the alignment

203

results showed that the efficiency of read alignment for the reads of each sample and the

204

reference genome ranged between 79.42% and 81.92% (*Table 1*), which guaranteed that the

205

selected reference genome assembly was qualified for data analysis.

206

Qualified transcriptome libraries are a major requisite for transcriptome sequencing. To ensure

207

the quality of the libraries, quality of the transcriptome sequencing libraries was evaluated from

208

three different perspectives:

209

(1) Randomicity of mRNA fragmentation and the degradation of mRNA were evaluated by

210

examining the distribution of inserted fragments in genes. As shown in *Figure S1*, The

211

degradation of mRNAs was relatively low in the 6 groups of samples.

212

213   (2) The dispersion degree of the inserted fragment length directly reflected the efficiency of

214   magnetic bead purification during library preparation. Simulated distribution of the inserted

215   fragment length for each sample showed only single-peak pattern, indicating a high purification

216   rate (*Fig. S2*).

217   (3) With the increase of sequencing data, the number of DEGs tended to saturate, as shown in

218   *Figure S3*, which confirmed that the data were sufficient and qualified for the subsequent

219   analysis.

220   ***DEG and DEGs Function annotation***

221   To acquire the comprehensive genetic information of ZBTB38$^{-/-}$ SH-SY5Y cells, the unigenes

222   were blasted against the NR, Swiss-Prot, GO, COG, KOG, Pfam, KEGG database resources to

223   identity the functions of all of the unigene sequences. All of DEGs were annotated to genes

224   having known functions in the indicated databases based on the sequences with the greatest

225   similarity. DEseq was used to analyze the DEGs derived from the two groups of cells to obtain a

226   DEGs set. Finally, a total of 2,036 (83.5%) down-regulated DEGs and 402 (16.5%) up-regulated

227   DEGs were selected. The number of DEGs annotated in this gene set was shown in *Table 2*.

228   A total of 2,258 (93.4%) DEGs were annotated successfully by GO annotation. These annotated

229   DEGs were classified into the next terms of three ontologies: BP (biological process), CC

230   (cellular component) and MF (molecular function). The distribution of unigenes is shown in

231   *Figure 4*. Among the "Biological Process", a high percentage of genes were classified into

232   Cellular Process (1,924 unigenes, 85.2%). Within the cellular component category, the majority

233   of genes were assigned into Cell Part (2,145 unigenes, 95%) . For the molecular function, most

234   of genes were involved in "Binding" (1,949 unigenes, 86.3%). The greatest number of annotated

235   unigenes were involved in Biological Process. The results of the topGO functional enrichment

236   analyses of DEGs indicated that the most significantly enriched GO terms focus on

237   "neurotrophin TRK receptor signaling pathway" (*Table S2*).

238   The unigenes was blasted against the COG database in order to orthologously classify gene

239   products. COG classification statistical results of DEGs were shown in *Figure 5*. In addition to

240   "General function prediction only", "Replication, recombination and repair" accounted for the

241   largest proportion of unigenes (180 DEGs, 13.06%), followed by "Transcription" (133 DEGs,

242   9.65%), "Signal transduction mechanisms"(128 DEGs, 9.29%), "Translation, ribosomal structure

243   and biogenesis" (80 DEGs, 5.81%), "Posttranslational Modification, Protein Turnover and

244   Chaperones" (79 DEGs, 5.73%), "cell cycle control, cell division, and chromosome partitioning"

245   (44 DEGs, 2.98%). According to the annotation results of the DEGs KEGG database, the largest

246   proportion of the unigenes were involved in the "MAPK signaling pathway" and "PI3K-Akt

247   signaling pathway" of "Environmental Information Processing"(*Figure 6*).

248 Based on the results above, a large number of DEGs were screened after a comparative analysis

249 of relevant databases. Meanwhile, functional annotation was also carried out that was crucial for

250 the further understanding of the cellular functions of ZBTB38 gene as a transcription factor.

251 ***Detection of candidate genes and analysis of the results of Real-time quantitative PCR***

252 Taking FPKM as a measure for the level of transcripts or gene expressions, DEGs in the p53

253 signaling pathway, including CDK4/6, Cyclin E, MDM2, ATM, ATR, PTEN, were down-

254 regulated, and Gadd45 and PIGs were up-regulated. Top 20 down-regulated unigenes associated

255 with autophagy were selected (*Table S3*), among which PIK3C2A was the most down-regulated

256 one, followed by RB1CC1 gene. In summary, the transcription factor ZBTB38 is involved in the

257 process of protein synthesis and also, as a positive regulatory factor, in the occurrence of

258 autophagy directly.

259 To validate the sequencing results obtained by RNA-seq, real-time quantitative PCR was

260 performed on three candidate genes, including PIK3C2A, RB1CC1, ATM, related to the mTOR

261 signaling pathway. The result showed that the expression of these candidate genes was

262 significantly decreased in the ZBTB38$^{-/-}$ cells compared to control group, which was similar to

263 the RNA-seq data (*Fig. 7*). The result verified the reliability of the transcription sequencing

264 results.

265

DISCUSSION

267 Transcriptomic studies are developing rapidly over recent years. Based on the information of the

268 whole mRNAs obtained in one cell or tissue, transcriptomic studies provide data on the

269 expression regulation systems and protein functions of all genes. NGS facilitates the deep

270 sequencing of whole cancer genomes for the discovery of novel therapeutic biomarkers, helping

271 to consequently build a solid foundation for comprehensive studies of cancer pharmacogenetics.

272 Furthermore, NGS allows for detailed analyses of the whole epigenome and transcriptome, thus

273 profoundly revealing the multilevel regulation networks of the human genome (McGettigan

274 2013; Wang et al. 2009; Young et al. 2010). Remarkably, the large amount of data information

275 of gene expression profiles revealed by transcriptome sequences have provided valuable

276 resources for studies investigating therapeutic biomarkers of cancer.

277 Genomic instability is an important factor in the early stages of cell carcinogenesis. Error-prone

278 DNA repair and the accumulation of abnormal DNA after repair are the main causes of genomic

279 instability (Lord & Ashworth 2012). Strict regulation of gene transcription is an essential factor

280 to maintain genomic stability (Kakarougkas et al. 2014). According to the statistical analysis of

281 the TCGA database, ZBTB protein family is mainly involved in the regulation of the expression

282 of target genes. Besides, the amplification, deficiency and/or mutation of most genes in ZBTB

283 family occurs in different types of tumors (Jardin et al. 2007; Maeda et al. 2007; Phan & Dalla-

284 Favera 2004). Among them, the expression changes of ZBTB38 gene are closely related to the

285 occurrence of 20 kinds of cancers (*Fig. 1A*), and there exists significant different expression

286 changes in different tumors, especially the most remarkable down-regulated expression in UCEC

287 and CESC (*Fig. 1B and D*). In our study, the statistical analysis of the prognosis of the LGG

288 patients exhibited a negative correlation with the expression change of ZBTB38 (*Fig. 2*),

289 indicating great significant concerning the study of the effect of ZBTB38 expression changes on

290 the occurrence and development of neuroma. However, there was no relevant report about the

291 expression change of ZBTB38 in NBs. This study demonstrated for the first time in vitro that the

292 knockdown of ZBTB38 seriously affected the proliferation of NB cells. Accordingly, it deserves

293 further analysis regarding the biological function of ZBTB38 and relationship with clinical

294 prognosis of NB.

295 Annotation of the function of the DEGs revealed that the most of DEGs after ZBTB38

296 knockdown enriched in neurotrophin TRK (tyrosine kinase receptor) receptor signaling pathway.

297 Neurotrophic factors (NTs) are a class of factors that regulate neuronal development,

298 differentiation, and function. NTs may activate two types of receptors, the high-affinity tyrosine

299 kinase family TRK receptors and the low-affinity p75NTR (p75 neurotrophin receptor)receptor

300 of the tumor necrosis factor receptor superfamily (Yang et al. 2016). NTs can initiate many

301 complex signal transduction pathways by activating these two types of receptors and thus exert

302 biological effects. In most cases, p75NTR is a ligand-activated apoptotic receptor, whose main

303 biological effect is to induce neuronal apoptosis and activate the apoptotic signal transduction

304 pathway JKN-p53-Bax (Redden et al. 2014). TRKs mainly activate two pathways: the PI3K-Akt

305 signaling pathway that inhibit the production and activity of apoptotic proteins, and the MAPK

306 signaling pathway that activate anti-apoptotic proteins to promote survival (Wong et al. 1999). In

307 this study, the KEGG pathway enrichment analysis of differentially expressed genes revealed

308 that DEGs were the most enriched genes in the MAPK and PI3K-Akt signaling pathways, and

309 most of the DEGs were downregulated, so we speculated that ZBTB38 knockdown-induced

310 reduction in viability and proliferation rate of SH-SY5Y cells may be closely related to these

311 pathways, and plan to focus on key components of the DEGs in future studies, to clarify the

312 molecular mechanism and to further evaluate the potential of ZBTB38 as a target gene to treated

313 NB.

314 A key feature of neuroblastoma is that it is uniformly p53 wild-type at diagnosis with intact

315 intrinsic and extrinsic apoptotic mechanisms, and direct inactivating p53 mutations are rare

316 regardless of stage of treatment suggests that neuroblastoma has an innate requirement for

317   baseline p53 activity (Kim & Shohet 2009). In the present study, the KEGG pathway enrichment
318   analysis of DEGs revealed that genes in the p53 signaling pathway, including CDK4/6, Cyclin E,
319   MDM2, ATM, ATR, PTEN, were down-regulated, and Gadd45 and PIGs were up-regulated
320   after the knockdown of ZBTB38 (*Fig. 8*). Both the CDK4/6-Cyclin D and the CDK2-Cyclin E
321   complexes are the central links in cell cycle regulation via regulating the G1-S transitions in
322   cells, and abnormal activation of the CyclinD-CDK4/6–INK4–Rb pathway, which is often
323   observed in various malignancies, will lead to uncontrolled growth of cancer cells (Sawai et al.
324   2012; The et al. 2015; VanArsdale et al. 2015). In addition, members of the Gadd45 family serve
325   as key regulatory genes in DNA damage repair pathway with p53 as the central link, and the
326   upregulation of Gadd45 plays an important role in the regulation of G2/M cell cycle checkpoints
327   and the maintenance of genomic stability, therefore to inhibit the cell transformation and the
328   malignant progression of tumors (Wang et al. 1999). ATM and ATR belong to the inositol
329   trisphosphate kinase family, both of which can be activated by DNA damage to phosphorylate
330   the downstream substrates such as CHK1, CHK2, and p53. In addition, the down-regulation of
331   both kinases may impair the downstream transmission of the molecular signals and inhibit the
332   p53 activity (Abraham 2001; Matsuoka et al. 2007). MDM2 regulates the function of p53 via
333   two approaches, i.e., mediating p53 degradation and inhibiting its transcriptional activity. As a
334   negative feedback regulator of p53, the inhibited expression of MDM2 can enhance the
335   transcriptional activity of p53 and inhibit tumorigenesis (Shangary & Wang 2009). PIGs is a
336   target downstream gene of p53 for the regulation of apoptosis, which is critical for cell apoptosis
337   by participating in the synthesis of reactive oxygen species and the regulation of oxidative stress
338   (Jin et al. 2017; Lee et al. 2010). When ZBTB38 gene is knocked down, more PIGs are
339   transferred into the nucleus where cell damage is repaired. Therefore, cellular response to DNA
340   damage is increased and the p53 induced ROS production, ultimately promote the apoptosis of
341   tumor cells. PTEN is a tumor suppressor gene with phosphatase activity. It is an upstream
342   regulatory inhibitor of the PI3K/Akt signal transduction pathway. PTEN is often referred to as a
343   "switch" molecule in the PI3K/Akt pathway due to its ability, which depends on its lipid
344   phosphatase activity, to remove the phosphate group and participate in the regulation of cell
345   activity. Once the expression of PTEN protein is reduced, the dephosphorylation of PIP3(the
346   lipid product of PI3-kinaseis) decreased. Excessive PIP3 is subsequently accumulated in the cells
347   and the PI3K/Akt signaling pathway is continuously activated, eventually leading to cell
348   proliferation or uncontrolled apoptosis and finally the occurrence of various diseases (Bleau et al.
349   2009; Carnero et al. 2008). In summary, studies that interrogating the roles of ZBTB38 and p53
350   pathways in growth and apoptosis of NB cells and those involving intervention of specific
351   signaling pathways may allow us to further understand the mechanisms of NB occurrence and
352   progression, and thus better evaluate and control this pediatric malignancy.

353   Majority of the DEGs were enriched in the PI3K-Akt signaling pathway among all KEGG
354   pathway enrichment categories, especially for those down-regulated genes, with most
355   significance noted in PIK3C2A and RB1CC1. PIK3C2A is a member of the PI3Ks family and
356   one of the key molecules in the signal transduction pathway of growth factors. It has been
357   reported that the overexpressed PIK3C2A in cells induces the accumulation and assembly of
358   clathrin, which mediates the transport of proteins between cell membranes and the network
359   structure of the Golgi body via regulating the movement of microtubules (Dragoi & Agaisse
360   2015; Shi et al. 2016). RB1CC1 (also known as FIP200) is an interacting protein of the focal
361   adhesion kinase family, with a molecular weight of 200kD. As documented in prior studies,
362   autophagy induction is abolished in RB1CC1-deficient cells. RB1CC1 is an important regulatory
363   protein that can acts on the autophagic initiation complex along with the ULK1 (Unc-51 like
364   autophagy activating kinase) simultaneously. Besides, it is also a key autophagy initiation factor
365   in the mTORC1-dependent signaling pathway (Ganley et al. 2009; Wang et al. 2011; Wei et al.
366   2009). Therefore, it is believed in our study that the autophagy regulation mechanism of the
367   mTORC1-dependent signaling pathway is also inhibited after ZBTB38 knockdown.
368   Orthologous assignments of gene products were carried out using the COG database.
369   Corresponding statistical analysis of the results also indicated that the silencing of ZBTB38 gene
370   affected the homeostasis of the whole cell, and as a transcriptional factor, ZBTB38 regulated the
371   transcription of intracellular proteins and influenced the expression and transport of proteins in
372   the downstream signaling pathways. The GO functional enrichment analyses of DEGs suggested
373   that most of the genes were involved in "Binding" and "Catalytic Activity" of the molecular
374   function between ZBTB38$^{-/-}$ cells and the controls. Therefore, this also partially explained the
375   biological functions of the key candidate genes enriched in KEGG pathway, i.e., all of them were
376   specific binding DNAs or proteins that regulated the transcriptional activity of target genes and
377   involved in various intracellular signaling pathways.

CONCLUSIONS

379   The functional knockdown of transcription factor ZBTB38 effectively inhibited proliferation and
380   differentiation of NB cells, which may be largely attributed to significant inhibition of the
381   neurotrophin TRK receptor signaling pathway. In addition, downregulation of ZBTB38 may also
382   promote apoptosis of the NB cells by regulating key components of the p53 signaling pathway.
383   Two DEGs closely related to autophagy initiation (PIK3C2A and RB1CC1) were significantly
384   inhibited, suggesting that ZBTB38 downregulation also blocked autophagy, an important
385   mechanism that protects the cells from programmed cell death, thus accelerating apoptosis of

386   tumor cells. The present meeting provides evidence to molecular mechanism of ZBTB38

387   modulating neuroblastoma development and targeted anti-tumor therapies.

388   ACKNOWLEDGEMENTS

389   This work was supported by the National Natural Science Foundation of China under Grant

390   [NSFC31372207 and 81570094]; the Innovation Team of Scientific Research Platform in Anhui

391   Province, a start-up Grant from Nanjing Agricultural University [804090].

392   REFERENCES

393   Abraham RT. 2001. Cell cycle checkpoint signaling through the ATM and ATR kinases. *Genes Dev*
394   15:2177-2196. 10.1101/gad.914401

395   Anders S, and Huber W. 2010. Differential expression analysis for sequence count data. *Genome Biol*
396   11:R106. 10.1186/gb-2010-11-10-r106

397   Bagatell R, and Cohn SL. 2016. Genetic discoveries and treatment advances in neuroblastoma. *Curr Opin*
398   *Pediatr* 28:19-25. 10.1097/MOP.0000000000000296

399   Binkhathlan Z, and Lavasanifar A. 2013. P-glycoprotein inhibition as a therapeutic approach for
400   overcoming multidrug resistance in cancer: current status and future perspectives. *Curr Cancer*
401   *Drug Targets* 13:326-346.

402   Bleau AM, Hambardzumyan D, Ozawa T, Fomchenko EI, Huse JT, Brennan CW, and Holland EC. 2009.
403   PTEN/PI3K/Akt pathway regulates the side population phenotype and ABCG2 activity in glioma
404   tumor stem-like cells. *Cell Stem Cell* 4:226-235. 10.1016/j.stem.2009.01.007

405   Cai Y, Li J, Yang S, Ping L, Xuan Z, and Liu H. 2012. CIBZ, a Novel BTB Domain-Containing Protein,
406   Is Involved in Mouse Spinal Cord Injury via Mitochondrial Pathway Independent of p53 Gene.
407   *PLoS One* 7:e33156. 10.1371/journal.pone.0033156

408   Cai Y, Li J, Zhang Z, Chen J, Zhu Y, Li R, Chen J, Gao L, Liu R, and Teng Y. 2017. Zbtb38 is a novel
409   target for spinal cord injury. *Oncotarget* 8:45356-45366. 10.18632/oncotarget.17487

410   Carnero A, Blanco-Aparicio C, Renner O, Link W, and Leal JF. 2008. The PTEN/PI3K/AKT signalling
411   pathway in cancer, therapeutic implications. *Curr Cancer Drug Targets* 8:187-198.

412   Castel V, Segura V, and Berlanga P. 2013. Emerging drugs for neuroblastoma. *Expert Opin Emerg Drugs*
413   18:155-171. 10.1517/14728214.2013.796927

414   Chang Z, Li G, Liu J, Zhang Y, Ashby C, Liu D, Cramer CL, and Huang X. 2015. Bridger: a new
415   framework for de novo transcriptome assembly using RNA-seq data. *Genome Biol* 16:30.
416   10.1186/s13059-015-0596-2

417   Dragoi AM, and Agaisse H. 2015. The class II phosphatidylinositol 3-phosphate kinase PIK3C2A
418   promotes Shigella flexneri dissemination through formation of vacuole-like protrusions. *Infect*
419   *Immun* 83:1695-1704. 10.1128/IAI.03138-14

420   Ewing B, and Green P. 1998. Base-calling of automated sequencer traces using phred. II. Error
421   probabilities. *Genome Res* 8:186-194.

422   Ewing B, Hillier L, Wendl MC, and Green P. 1998. Base-calling of automated sequencer traces using
423   phred. I. Accuracy assessment. *Genome Res* 8:175-185.

424 Florea L, Song L, and Salzberg SL. 2013. Thousands of exon skipping events differentiate among
425   splicing patterns in sixteen human tissues. *F1000Res* 2:188. 10.12688/f1000research.2-188.v2
426 Ganley IG, Lam du H, Wang J, Ding X, Chen S, and Jiang X. 2009. ULK1.ATG13.FIP200 complex
427   mediates mTOR signaling and is essential for autophagy. *J Biol Chem* 284:12297-12305.
428   10.1074/jbc.M900573200
429 Gotz S, Garcia-Gomez JM, Terol J, Williams TD, Nagaraj SH, Nueda MJ, Robles M, Talon M, Dopazo J,
430   and Conesa A. 2008. High-throughput functional annotation and data mining with the Blast2GO
431   suite. *Nucleic Acids Res* 36:3420-3435. 10.1093/nar/gkn176
432 Han W, and Wang HM. 2015. Refractory diarrhea: A paraneoplastic syndrome of neuroblastoma. *World J*
433   *Gastroenterol* 21:7929-7932. 10.3748/wjg.v21.i25.7929
434 Jardin F, Ruminy P, Bastard C, and Tilly H. 2007. The BCL6 proto-oncogene: a leading role during
435   germinal center development and lymphomagenesis. *Pathol Biol (Paris)* 55:73-83.
436   10.1016/j.patbio.2006.04.001
437 Jin M, Park SJ, Kim SW, Kim HR, Hyun JW, and Lee JH. 2017. PIG3 Regulates p53 Stability by
438   Suppressing Its MDM2-Mediated Ubiquitination. *Biomol Ther (Seoul)* 25:396-403.
439   10.4062/biomolther.2017.086
440 Kakarougkas A, Ismail A, Chambers AL, Riballo E, Herbert AD, Kunzel J, Lobrich M, Jeggo PA, and
441   Downs JA. 2014. Requirement for PBAF in transcriptional repression and repair at DNA breaks
442   in actively transcribed regions of chromatin. *Mol Cell* 55:723-732. 10.1016/j.molcel.2014.06.028
443 Kanehisa M, Araki M, Goto S, Hattori M, Hirakawa M, Itoh M, Katayama T, Kawashima S, Okuda S,
444   Tokimatsu T, and Yamanishi Y. 2008. KEGG for linking genomes to life and the environment.
445   *Nucleic Acids Res* 36:D480-484. 10.1093/nar/gkm882
446 Kim D, Pertea G, Trapnell C, Pimentel H, Kelley R, and Salzberg SL. 2013. TopHat2: accurate alignment
447   of transcriptomes in the presence of insertions, deletions and gene fusions. *Genome Biol* 14:R36.
448   10.1186/gb-2013-14-4-r36
449 Kim E, and Shohet J. 2009. Targeted molecular therapy for neuroblastoma: the ARF/MDM2/p53 axis. *J*
450   *Natl Cancer Inst* 101:1527-1529. 10.1093/jnci/djp376
451 Langmead B, Trapnell C, Pop M, and Salzberg SL. 2009. Ultrafast and memory-efficient alignment of
452   short DNA sequences to the human genome. *Genome Biol* 10:R25. 10.1186/gb-2009-10-3-r25
453 Lee JH, Kang Y, Khare V, Jin ZY, Kang MY, Yoon Y, Hyun JW, Chung MH, Cho SI, Jun JY, Chang IY,
454   and You HJ. 2010. The p53-inducible gene 3 (PIG3) contributes to early cellular response to
455   DNA damage. *Oncogene* 29:1431-1450. 10.1038/onc.2009.438
456 Lee SU, and Maeda T. 2012. POK/ZBTB proteins: an emerging family of proteins that regulate lymphoid
457   development and function. *Immunol Rev* 247:107-119. 10.1111/j.1600-065X.2012.01116.x
458 Li B, Fillmore N, Bai Y, Collins M, Thomson JA, Stewart R, and Dewey CN. 2014. Evaluation of de
459   novo transcriptome assemblies from RNA-Seq data. *Genome Biol* 15:553. 10.1186/s13059-014-
460   0553-5
461 Lord CJ, and Ashworth A. 2012. The DNA damage response and cancer therapy. *Nature* 481:287-294.
462   10.1038/nature10760
463 Maeda T, Merghoub T, Hobbs RM, Dong L, Maeda M, Zakrzewski J, van den Brink MR, Zelent A,
464   Shigematsu H, Akashi K, Teruya-Feldstein J, Cattoretti G, and Pandolfi PP. 2007. Regulation of

465   B versus T lymphoid lineage fate decision by the proto-oncogene LRF. *Science* 316:860-866.
466   10.1126/science.1140881
467   Mao X, Cai T, Olyarchuk JG, and Wei L. 2005. Automated genome annotation and pathway
468   identification using the KEGG Orthology (KO) as a controlled vocabulary. *Bioinformatics*
469   21:3787-3793. 10.1093/bioinformatics/bti430
470   Matsuda E, Yu O, and Kawaichi M. 2008. CIBZ,a BTB-containing Zinc Finger Protein,Plays a Role in
471   Apoptosis and Tumorigenesis. bit life sciences' 1st annual world cancer congess-2008.
472   Matsuoka S, Ballif BA, Smogorzewska A, McDonald ER, 3rd, Hurov KE, Luo J, Bakalarski CE, Zhao Z,
473   Solimini N, Lerenthal Y, Shiloh Y, Gygi SP, and Elledge SJ. 2007. ATM and ATR substrate
474   analysis reveals extensive protein networks responsive to DNA damage. *Science* 316:1160-1166.
475   10.1126/science.1140321
476   McGettigan PA. 2013. Transcriptomics in the RNA-seq era. *Curr Opin Chem Biol* 17:4-11.
477   10.1016/j.cbpa.2012.12.008
478   Nishii T, Oikawa Y, Ishida Y, Kawaichi M, and Matsuda E. 2012. CtBP-interacting BTB zinc finger
479   protein (CIBZ) promotes proliferation and G1/S transition in embryonic stem cells via Nanog.
480   *Journal of Biological Chemistry* 287:12417. 10.1074/jbc.M111.333856
481   Phan RT, and Dalla-Favera R. 2004. The BCL6 proto-oncogene suppresses p53 expression in germinal-
482   centre B cells. *Nature* 432:635-639. 10.1038/nature03147
483   Redden RA, Iyer R, Brodeur GM, and Doolin EJ. 2014. Rotary bioreactor culture can discern specific
484   behavior phenotypes in Trk-null and Trk-expressing neuroblastoma cell lines. *In Vitro Cell Dev*
485   *Biol Anim* 50:188-193. 10.1007/s11626-013-9716-z
486   Reimann E, Koks S, Ho XD, Maasalu K, and Martson A. 2014. Whole exome sequencing of a single
487   osteosarcoma case--integrative analysis with whole transcriptome RNA-seq data. *Hum Genomics*
488   8:20. 10.1186/s40246-014-0020-0
489   Robinson MD, McCarthy DJ, and Smyth GK. 2010. edgeR: a Bioconductor package for differential
490   expression analysis of digital gene expression data. *Bioinformatics* 26:139-140.
491   10.1093/bioinformatics/btp616
492   Sasai N, Matsuda E, Sarashina E, Ishida Y, and Kawaichi M. 2005. Identification of a novel BTB-zinc
493   finger transcriptional repressor, CIBZ, that interacts with CtBP corepressor. *Genes to Cells*
494   10:871–885. 10.1111/j.1365-2443.2005.00885.x
495   Sawai CM, Freund J, Oh P, Ndiaye-Lobry D, Bretz JC, Strikoudis A, Genesca L, Trimarchi T, Kelliher
496   MA, Clark M, Soulier J, Chen-Kiang S, and Aifantis I. 2012. Therapeutic targeting of the cyclin
497   D3:CDK4/6 complex in T cell leukemia. *Cancer Cell* 22:452-465. 10.1016/j.ccr.2012.09.016
498   Schulte JH, Schulte S, Heukamp LC, Astrahantseff K, Stephan H, Fischer M, Schramm A, and Eggert A.
499   2013. Targeted Therapy for Neuroblastoma: ALK Inhibitors. *Klin Padiatr* 225:303-308.
500   10.1055/s-0033-1357132
501   Shangary S, and Wang S. 2009. Small-molecule inhibitors of the MDM2-p53 protein-protein interaction
502   to reactivate p53 function: a novel approach for cancer therapy. *Annu Rev Pharmacol Toxicol*
503   49:223-241. 10.1146/annurev.pharmtox.48.113006.094723

504 Shi Y, Gao X, Hu Q, Li X, Xu J, Lu S, Liu Y, Xu C, Jiang D, Lin J, Xue A, Tan Y, Shen K, and Hou Y.
505   2016. PIK3C2A is a gene-specific target of microRNA-518a-5p in imatinib mesylate-resistant
506   gastrointestinal stromal tumor. *Lab Invest* 96:652-660. 10.1038/labinvest.2015.157
507 Stogios PJ, Downs GS, Jauhal JJ, Nandra SK, and Prive GG. 2005. Sequence and structural analysis of
508   BTB domain proteins. *Genome Biol* 6:R82. 10.1186/gb-2005-6-10-r82
509 The I, Ruijtenberg S, Bouchet BP, Cristobal A, Prinsen MB, van Mourik T, Koreth J, Xu H, Heck AJ,
510   Akhmanova A, Cuppen E, Boxem M, Munoz J, and van den Heuvel S. 2015. Rb and FZR1/Cdh1
511   determine CDK4/6-cyclin D requirement in C. elegans and human cancer cells. *Nat Commun*
512   6:5906. 10.1038/ncomms6906
513 VanArsdale T, Boshoff C, Arndt KT, and Abraham RT. 2015. Molecular Pathways: Targeting the Cyclin
514   D-CDK4/6 Axis for Cancer Treatment. *Clin Cancer Res* 21:2905-2910. 10.1158/1078-
515   0432.CCR-14-0816
516 Wang D, Olman MA, Stewart J, Jr., Tipps R, Huang P, Sanders PW, Toline E, Prayson RA, Lee J, Weil
517   RJ, Palmer CA, Gillespie GY, Liu WM, Pieper RO, Guan JL, and Gladson CL. 2011.
518   Downregulation of FIP200 induces apoptosis of glioblastoma cells and microvascular endothelial
519   cells by enhancing Pyk2 activity. *PLoS One* 6:e19629. 10.1371/journal.pone.0019629
520 Wang XW, Zhan Q, Coursen JD, Khan MA, Kontny HU, Yu L, Hollander MC, O'Connor PM, Fornace
521   AJ, Jr., and Harris CC. 1999. GADD45 induction of a G2/M cell cycle checkpoint. *Proc Natl*
522   *Acad Sci U S A* 96:3706-3711.
523 Wang Z, Gerstein M, and Snyder M. 2009. RNA-Seq: a revolutionary tool for transcriptomics. *Nat Rev*
524   *Genet* 10:57-63. 10.1038/nrg2484
525 Wei H, Gan B, Wu X, and Guan JL. 2009. Inactivation of FIP200 leads to inflammatory skin disorder,
526   but not tumorigenesis, in conditional knock-out mouse models. *J Biol Chem* 284:6004-6013.
527   10.1074/jbc.M806375200
528 Wong BR, Besser D, Kim N, Arron JR, Vologodskaia M, Hanafusa H, and Choi Y. 1999. TRANCE, a
529   TNF family member, activates Akt/PKB through a signaling complex involving TRAF6 and c-
530   Src. *Mol Cell* 4:1041-1049.
531 Yang T, Massa SM, Tran KC, Simmons DA, Rajadas J, Zeng AY, Jang T, Carsanaro S, and Longo FM.
532   2016. A small molecule TrkB/TrkC neurotrophin receptor co-activator with distinctive effects on
533   neuronal survival and process outgrowth. *Neuropharmacology* 110:343-361.
534   10.1016/j.neuropharm.2016.06.015
535 Young MD, Wakefield MJ, Smyth GK, and Oshlack A. 2010. Gene ontology analysis for RNA-seq:
536   accounting for selection bias. *Genome Biol* 11:R14. 10.1186/gb-2010-11-2-r14
537 Zhang Z, Chen J, Chen F, Yu D, Li R, Lv C, Wang H, Li H, Li J, and Cai Y. 2017. Tauroursodeoxycholic
538   acid alleviates secondary injury in the spinal cord via up-regulation of CIBZ gene. *Cell Stress*
539   *Chaperones*. 10.1007/s12192-017-0862-1
540 Zhao QY, Wang Y, Kong YM, Luo D, Li X, and Hao P. 2011. Optimizing de novo transcriptome
541   assembly from short-read RNA-Seq data: a comparative study. *BMC Bioinformatics* 12 Suppl
542   14:S2. 10.1186/1471-2105-12-S14-S2

543

Figure 1

Expression analysis of ZBTB38 gene in different tumors based on TCGA Database.

(A) The expression changes of ZBTB38 gene are closely related to the occurrence of 20 kinds of cancers; (B-D) ZBTB38 expression profiles based on top 4 cancer stages.

A

Cancer Distribution

B

Expression of ZBTB38 in UCEC based on major cancer stages

C

Expression of ZBTB38 in STAD based on major cancer stages

D

Expression of ZBTB38 in CESC based on major cancer stages

E

Expression of ZBTB38 in COAD based on major cancer stages
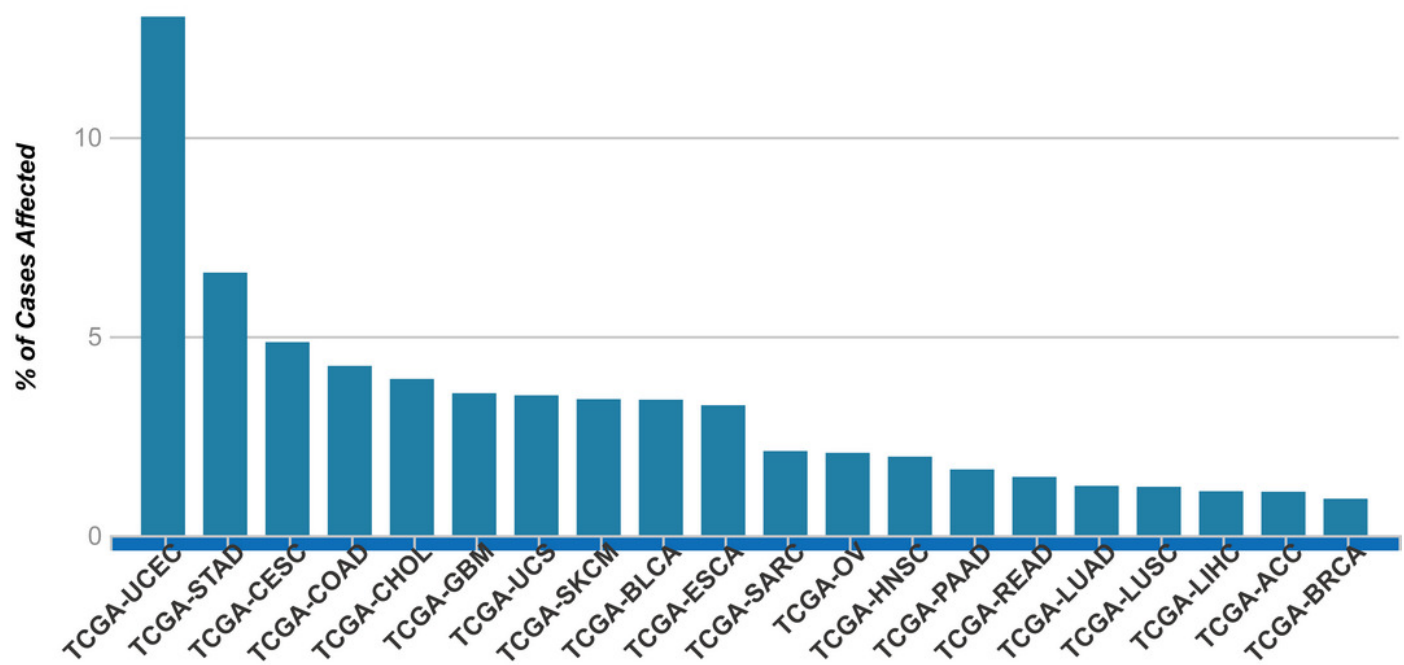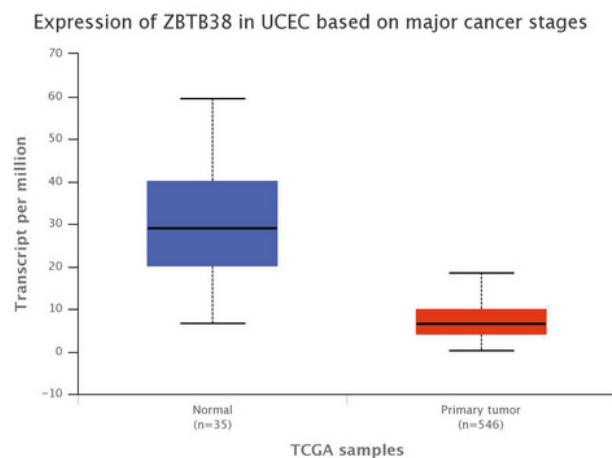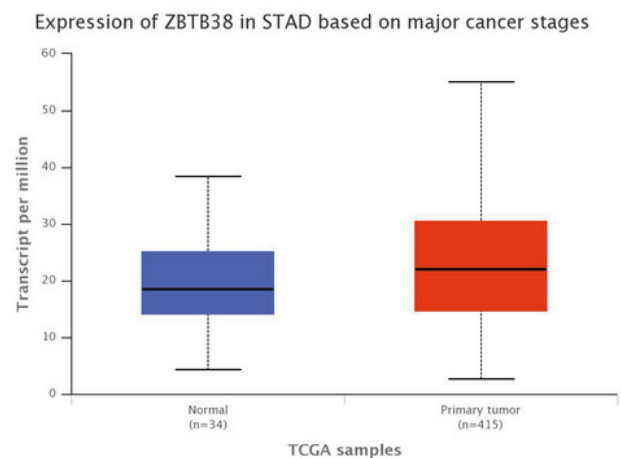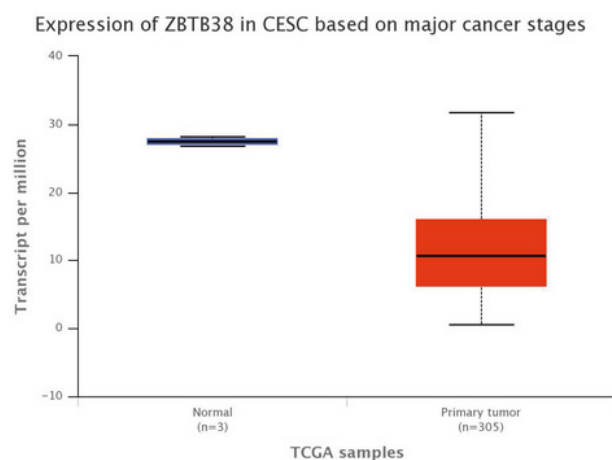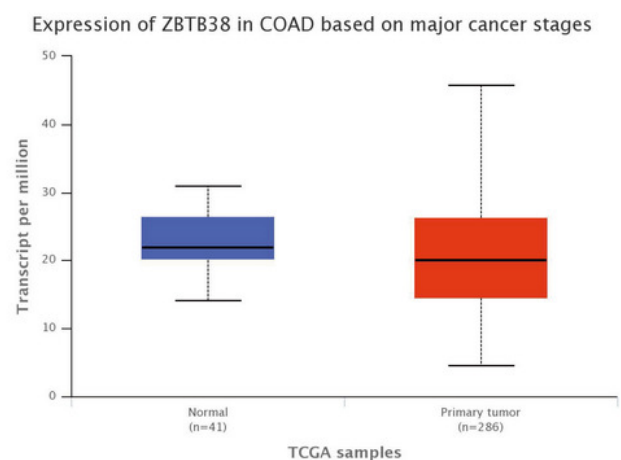
Figure 2

Effect of ZBTB38 expression level on LGG patient survival.

Red and blue lines indicated high and low expression groups, respectively. P = 0.02 < 0.05 was considered to be statistically significant.
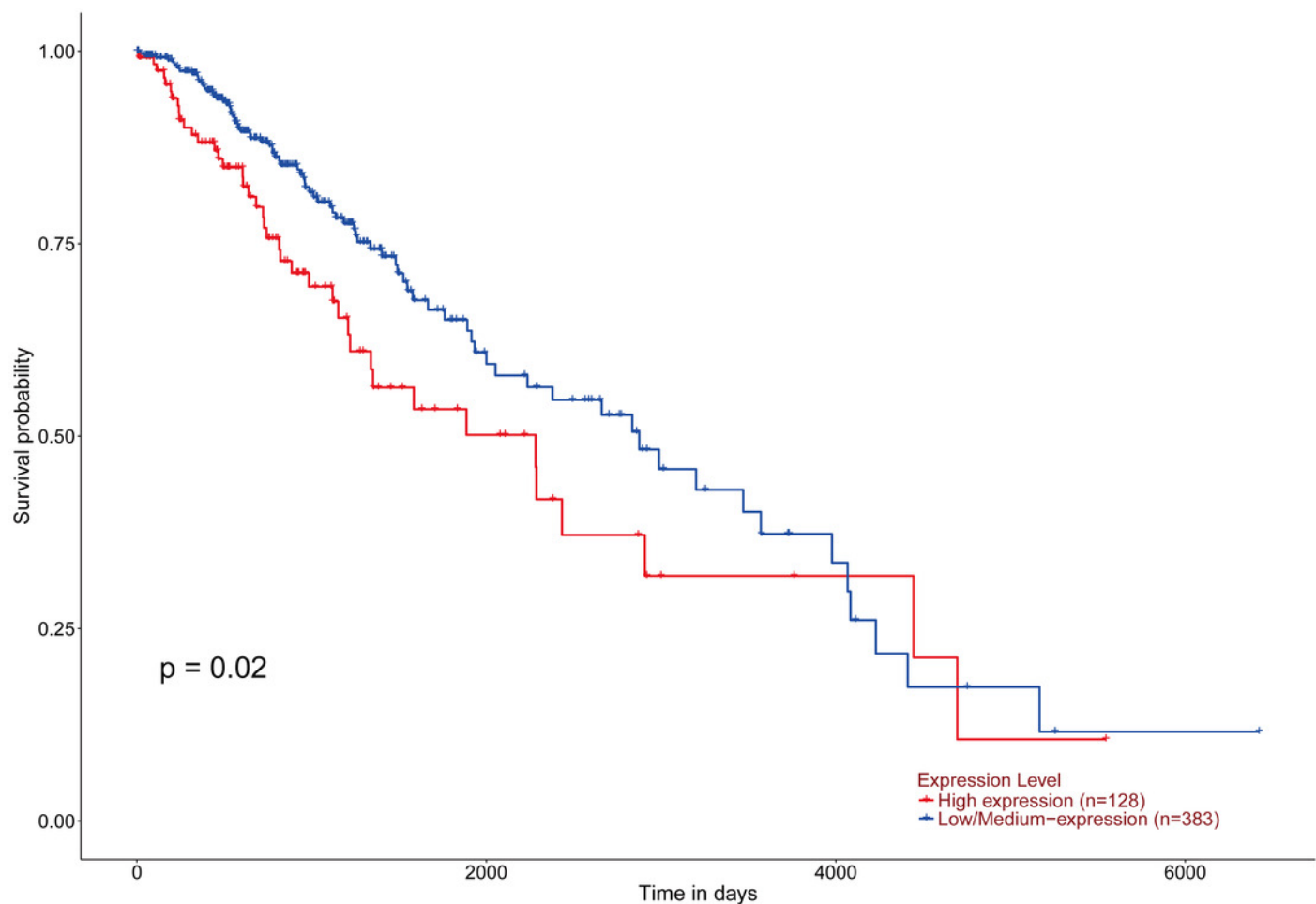
Figure 3

Proliferation and viability of ZBTB38 knockdown SH-SY5Y cells.

(A, B) SH-SY5Y cells were divided into two groups underwent control group and siRNA,
respectively. cell lysates were collected for Western blot analysis on the 24 h after
transfecting different sequences of ZBTB38 siRNAs (siRNA1, siRNA2 and siRNA3 indicate
three different siRNA primers). Representative images of these assays are shown in (A) and
quantitative data are shown in (B); β-actin was used as an internal control. SH-SY5Y cell
*proliferation (C) and viability (D) in different groups. *p<0.05. Data are presented as means*
± SEM from at least 3 independent experiments. Control, SH-SY5Y cells treated with
liposome alone; ZBTB38-/-, SH-SY5Y cells transfected with ZBTB38 siRNA.
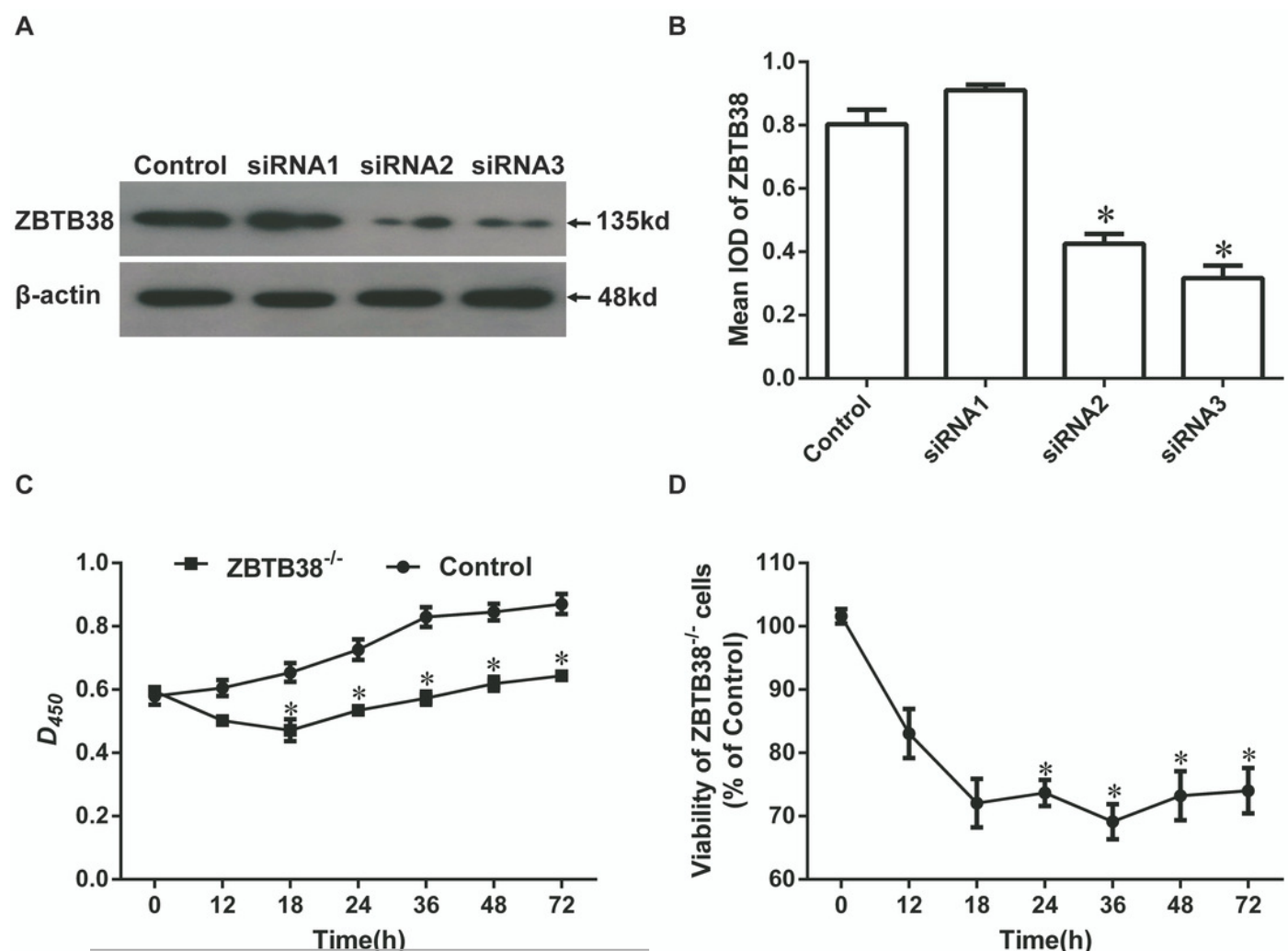
Figure 4

Gene function classification of all annotated unigenes by Gene Ontology.

The vertical axis represents the number of unigenes, and horizontal axis gives the specific GO sub-categories.
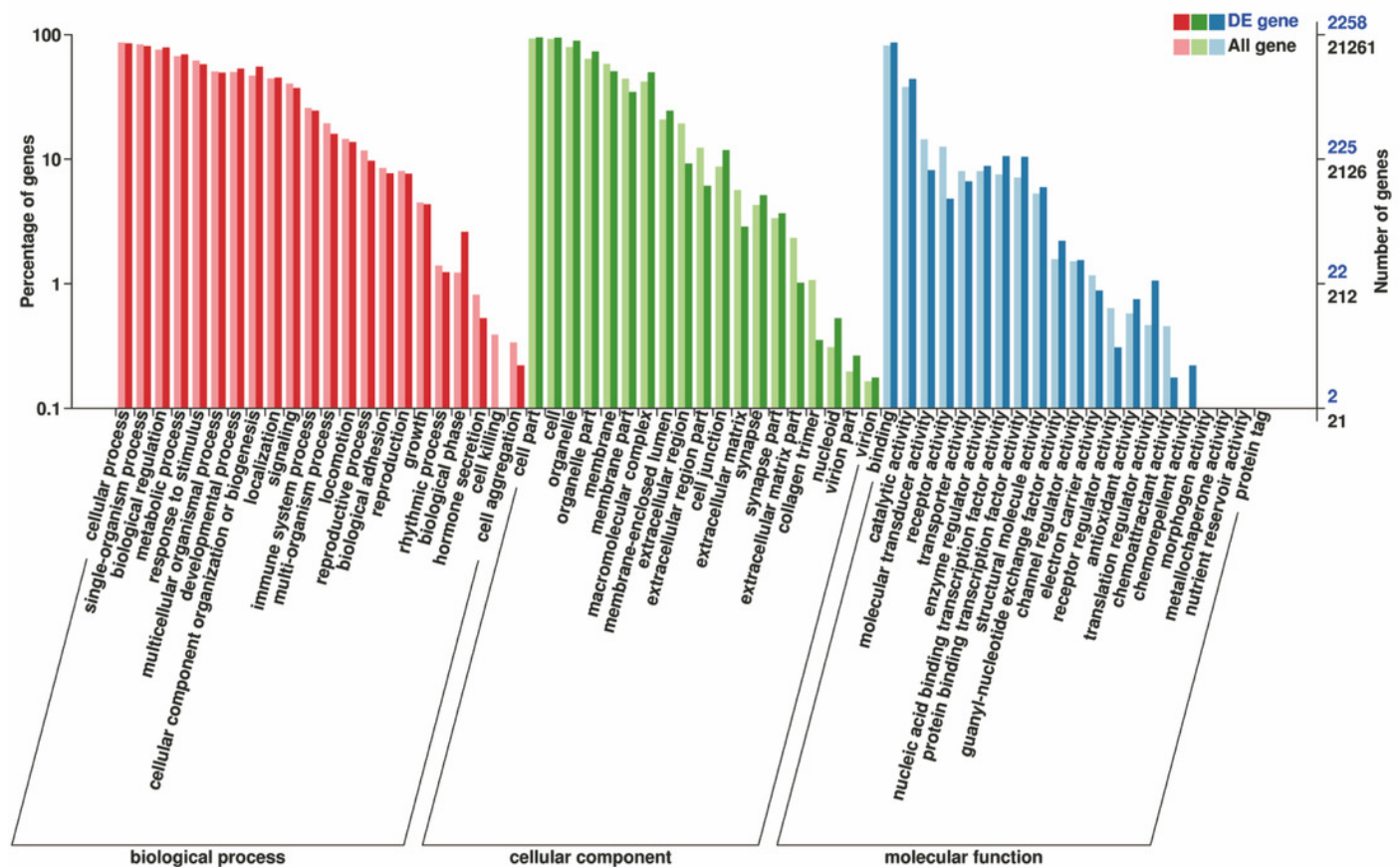
Figure 5

COG function classification of consensus sequence.

The vertical axis represents the frequency of unigenes classified into the specific categories, and horizontal axis gives the COG function classification.
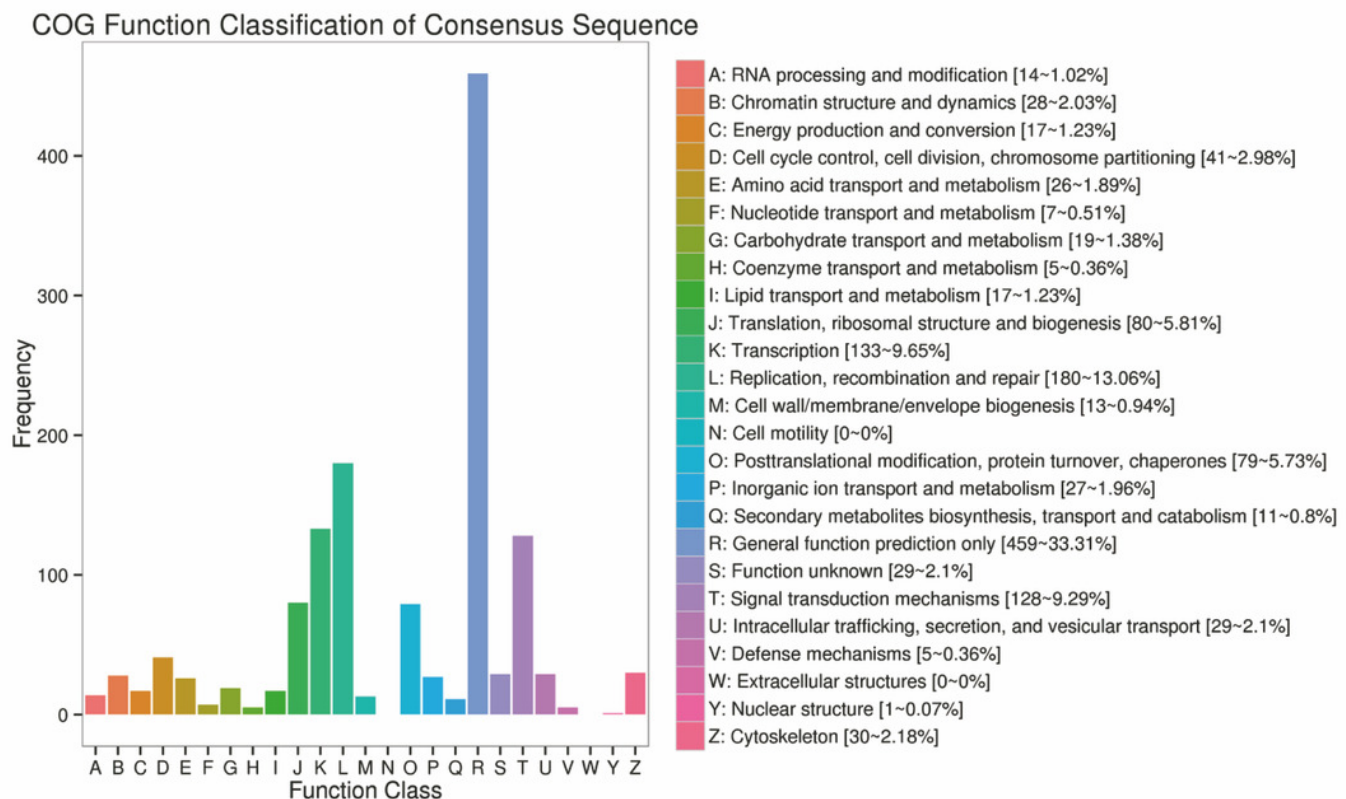
Figure 6

DEG KEGG classification.

The vertical axis lists the various metabolic pathways, and horizontal axis gives the number of annotated genes in the pathways.
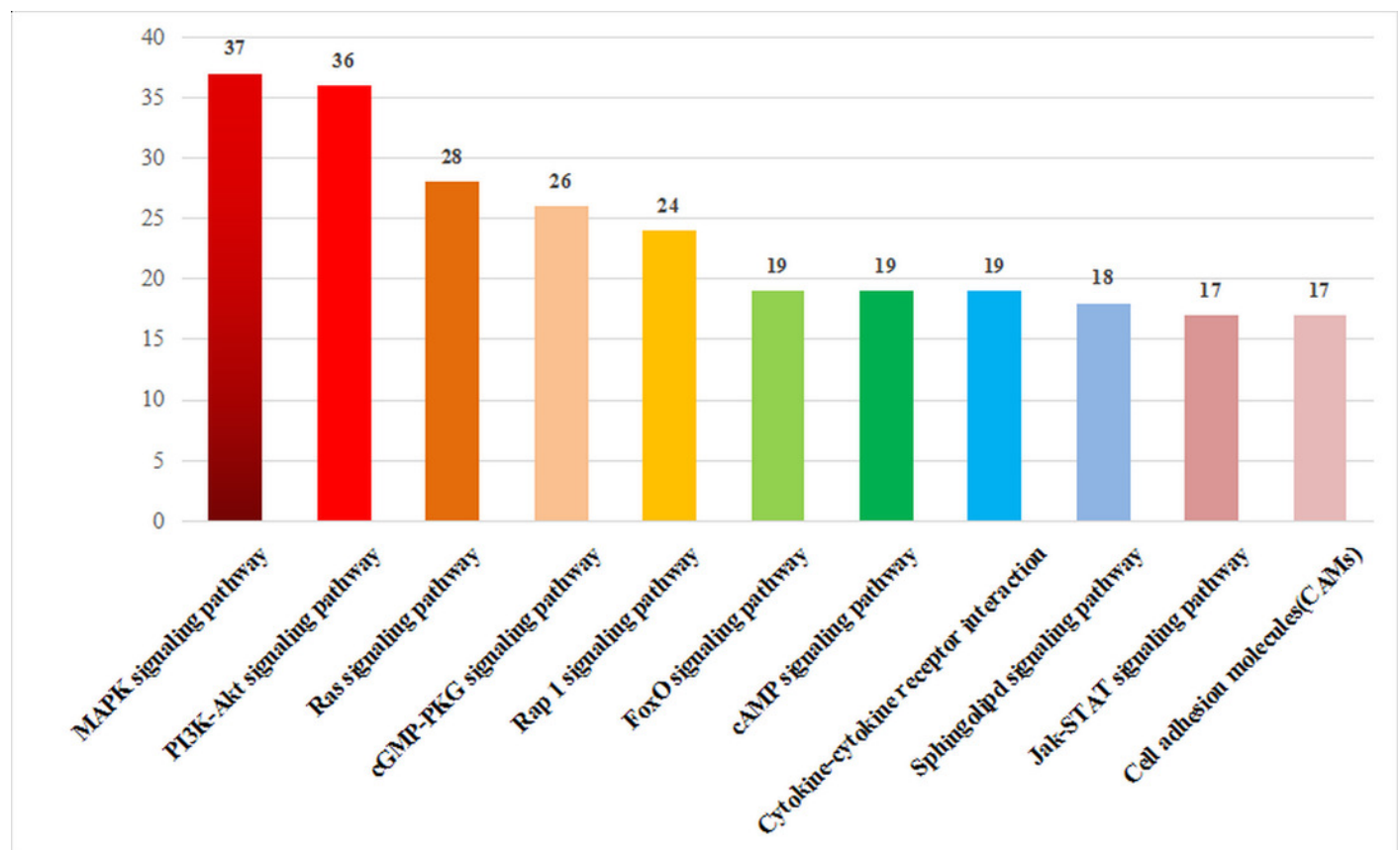
Figure 7

Differential expression analysis of candidate genes between ZBTB38$^{-/-}$ and ZBTB38 SH-SY5Y cells.

(A) The result of qRT-PCR. (B)The result of RNA-seq.
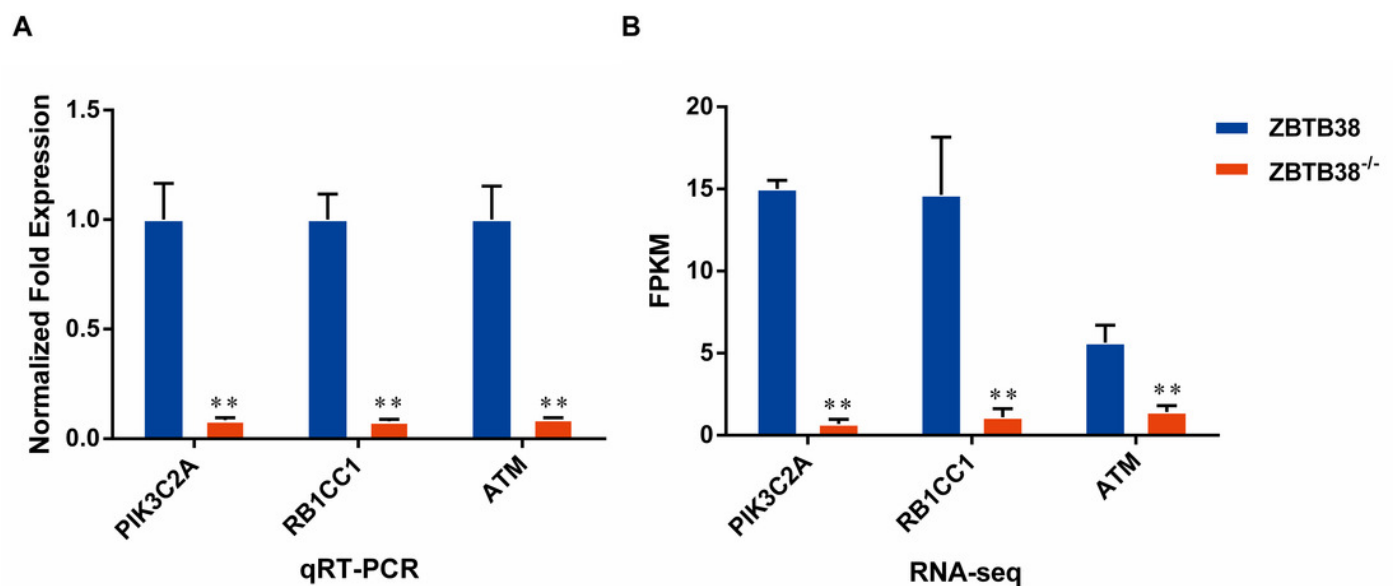
Figure 8

KEGG pathway annotation map of differentially expressed genes in p53 signaling pathway.

Relative to the control group, the red labeled protein was associated with the up-regulated gene and the white labeled protein was associated with the down-regulated gene.
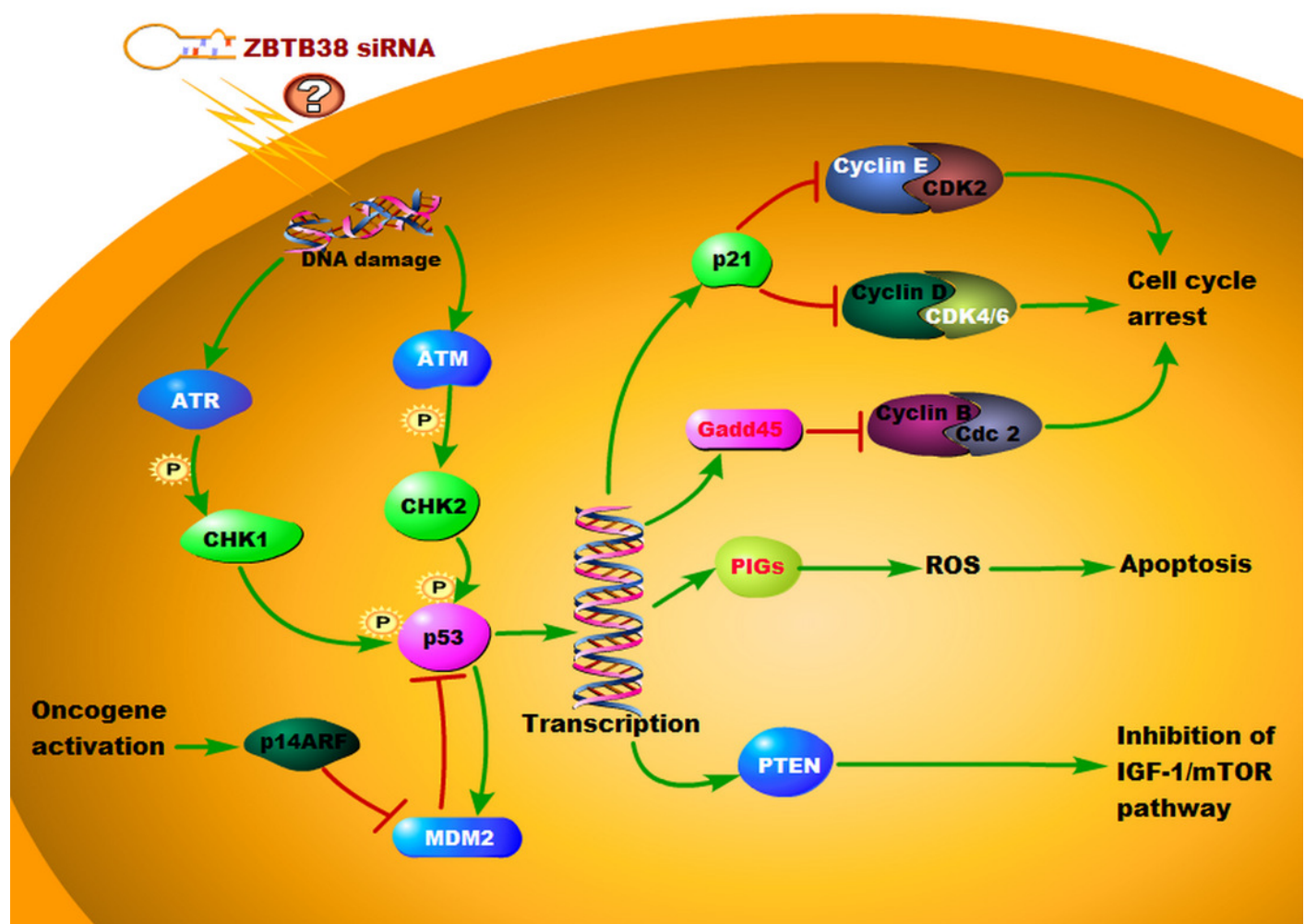
Summary of Sequence comparisons among sample sequencing data and selected reference genomes.

2 **Table 1. Summary of Sequence comparisons among sample sequencing data and selected reference genomes.**

Samples-ID	Total Reads	Mapped Reads	Uniq Mapped Reads	Multiple Map Reads	GC Content	%≥Q30
T01	41,320,306	32,993,483 (79.85%)	29,171,906 (70.60%)	3,821,577 (9.25%)	56.24%	89.44%
T02	53,706,092	42,655,511 (79.42%)	37,610,672 (70.03%)	5,044,839 (9.39%)	55.36%	89.45%
T04	54,889,928	44,964,104 (81.92%)	41,561,590 (75.72%)	3,402,514 (6.20%)	52.17%	90.04%
T05	50,160,236	40,559,313 (80.86%)	37,552,835 (74.87%)	3,006,478 (5.99%)	52.16%	90.25%
T06	62,721,676	50,526,963 (80.56%)	47,347,475 (75.49%)	3,179,488 (5.07%)	51.94%	90.05%
T07	54,693,534	43,544,178 (79.61%)	38,543,679 (70.47%)	5,000,499 (9.14%)	55.22%	89.30%

3 T01, T02, and T07 indicate the ZBTB38$^{-/-}$ SH-SY5Y cells. T04, T05, and T06 indicate the control groups. Total Reads: Number of Clean Reads,

4 single-ended; Mapped Reads: Number of Reads aligned to the reference genome and percentage in Clean Reads; Uniq Mapped Reads: Match The

5 number of Reads to the unique position of the reference genome and the percentage of the Clean Reads; Multiple Map Reads: The number of

6 Reads aligned to multiple locations in the reference genome and the percentage of Clean Reads.GC content: The Clean Data GC content; ≥ Q30% :

7 The percentage of bases with a Clean Data quality value ≥ 30.

Summary of the function annotation results for ZBTB38$^{-/-}$ unigenes in public protein databases.

1   **Table 2. Summary of the function annotation results for ZBTB38$^{-/-}$ unigenes in public protein**

2   **databases.**

DEG Set	Total	COG	GO	KEGG	KOG	NR	Swiss-Prot	eggNOG
T04_T05_T06 vs T01_T02_T07	2,417	999	2,258	1,512	1,733	2,337	2,377	2,405